Hollow core fiber Fabry-Perot interferometers with reduced sensitivity to temperature

MENG DING[1,*] ERIC NUMKAM FOKOUA[1], JOHN R. HAYES[1], HESHAM SAKR[1], PETER HORAK[1], FRANCESCO POLETTI[1], DAVID J. RICHARDSON[1], AND RADAN SLAVÍK[1]

[1]*Optoelectronics Research Centre, University of Southampton, Southampton, SO17 1BJ, UK*
**Corresponding author: m.ding@soton.ac.uk*

Received XX Month XXXX; revised XX Month, XXXX; accepted XX Month XXXX; posted XX Month XXXX (Doc. ID XXXXX); published XX Month XXXX

We demonstrate a 3x thermal phase sensitivity reduction for a hollow core fiber Fabry-Perot interferometer by winding the already low temperature sensitivity HCF on to a spool made from an ultralow thermal expansion material. A record low room temperature fiber coil phase thermal sensitivity of 0.13 ppm/K is demonstrated. The result is of particular interest in reducing the thermal sensitivity of HCF-based Fabry-Perot interferometers (for which existing thermal sensitivity reduction methods are not applicable). Our theoretical analysis predicts that significantly lower (or even zero) thermal sensitivity should be achievable when a spool with slightly negative coefficient of thermal expansion is used. We also suggest a method to fine-tune the thermal sensitivity and analyze it with simulations.

http://dx.doi.org/10.1364/OL.99.099999

Light inside Fabry-Pertot interferometers (FPI) travels many times between the two cavity mirrors, enabling long path lengths in a compact form. For example, vacuum-based FPI cavities with a finesse in excess of 100 000 are used in metrology [1] to reduce the noise of lasers. Such cavities are typically 10-50 cm long, enabling an 'equivalent' light path length of up to almost 150 km [2]. However, due to various technical reasons (i.e. mirror alignment accuracy and mirror quality requirements that increase rapidly with finesse) most FPIs based on light propagation between two mirrors in free space have a finesse of 100-1000, with associated effective light path lengths of up to hundreds of meters. An increase in the cavity round-trip time, reduction of the mirror alignment sensitivity, and less weight/volume can be achieved in fiber-based FPIs, where the mirrors are deposited directly on the end-facets of a single-mode fiber (SMF). A finesse in excess of 2000 has been demonstrated with fiber lengths of 10 m, enabling an equivalent path length of 20 km [3].

To achieve the highly stable operation required in applications such as laser stabilization [2], the FPIs' sensitivity to temperature must be managed. In free-space FPIs this is addressed, e.g., by fixing the distance between mirrors with materials with ultra-low or even zero-crossing coefficient of thermal expansion (CTE) such as silica glass [4], Invar, or ultra-low expansion (e.g., ULE) glass. For SMF-based FPIs, the thermal sensitivity is relatively large, as light propagates through the glass core, which has a relatively strong thermo-optic coefficient. This can be significantly reduced by using hollow core fiber (HCF) instead of SMF, as light propagates almost entirely through the empty core which is surrounded by a glass microstructure responsible for light guidance [5]. HCFs with attenuation levels close to that of SMF in the low-loss C-band (down to 0.22 dB/km, with attenuation even lower than for SMF at shorter wavelengths, e.g., below 1000 nm) were recently demonstrated [6]. Free-space coupled HCF-FPIs were demonstrated over >10 m lengths with finesse values > 1000, corresponding to effective path lengths of >10 km [7]. A 22-m long alignment-free (after fabrication) HCF-FPI with a finesse of over 120 and with the light coupled directly from an SMF has also been demonstrated [8], providing an effective path length of >2.5 km.

Although HCF-FPIs already have a thermal sensitivity about 15 times lower than SMF-FPIs of the same optical length [8], it is desirable to reduce it even further. As the thermal sensitivity of HCF is mostly given by the CTE of silica glass [5], reducing the thermal sensitivity of HCF-FPI's requires a reduction in the thermally-induced expansion of the HCF. Published approaches include operating at very low temperatures where the CTE of silica glass crosses zero [9, 10]. This was shown to occur at -71°C in uncoated HCF [9] and was predicted to occur at even lower temperatures for coated HCF [10] since standard acrylate fiber coating becomes very stiff at low temperatures, significantly altering the thermal expansion of the coated HCF. Another option is to use HCF with open ends, where changes in optical phase due to HCF elongation can be compensated by refractive index changes associated with pressure-driven ingress/egress of air to/from the central hole [11]. At atmospheric pressure, this allows for zero thermal sensitivity to be achieved close to 110°C. However, for many applications, operation at or close to room temperature is desired.

Here we elaborate on our preliminary work [12] in which we suggested a method to reduce the thermal sensitivity of a HCF-FPI at room temperature down to potentially zero. Our method is based on tightly winding the HCF-FPI on a spool made of a material with

zero or slightly negative CTE (such as Zerodur from Schott [13] or ULE glass from Corning [14]). As we show through simulations, although zero thermal sensitivity can in principle be achieved already with a zero-CTE spool, for coated HCF a slightly negative CTE of the spool is required. In our proof-of-principle demonstration, we reduced the HCF-FPI thermal sensitivity by a factor of three even with a spool with a small positive CTE, demonstrating a fiber FPI about 60 times less sensitive than a fiber FPI based on SMF. Although we demonstrate this on a FPI, the same approach can be used to reduce the thermal sensitivity of other interferometers based on HCF or HCF-based delay lines.

Our technique involves initial pre-stretching of the HCF at room temperature and fixing its stretched length (we explain later how we do this). We can visualize this by thinking of the length of HCF as a string on a guitar. When we heat the HCF/string up, the tension is reduced (due to temperature-induced elongation of the HCF/string, which then requires less force to keep it in the original elongated state). The string then plays at a lower pitch whilst maintaining its length. This keeps the HCF/string straight (under tension) as long as the heat-induced elongation is smaller than the original pre-stretching. The associated glass refractive index change through the stress-optic effect has negligible influence on the light guided through the HCF thanks to its propagation mostly through the air-filled core rather than the silica glass.

To fix the stretched HCF length, we coil the HCF under tension on a spool made of a very low or zero CTE material, Fig. 1 (a). We use Zerodur from Schott in our experiment, but there are several other materials with similar properties, e.g., ULE glass from Corning, ZERØ from Nippon, or IC-ZX from Shinhokoku. With increasing temperature, the spool maintains its size, forcing the HCF to maintain its length as well. The heating would have elongated a freely coiled HCF, but as it is under a stretch, it only reduces the tensile force, meaning the length is fully-dictated by the spool size. In this way, the CTE of the HCF should be identical to the CTE of the spool. Silica glass from which HCF is made has CTE = 3×10^{-7}/K [15], meaning that a 100 K temperature change would change its length by 0.003%. Fibers can be stretched significantly more (usually proof-tested at 0.5 or 1%), making our technique applicable over a very broad temperature range.

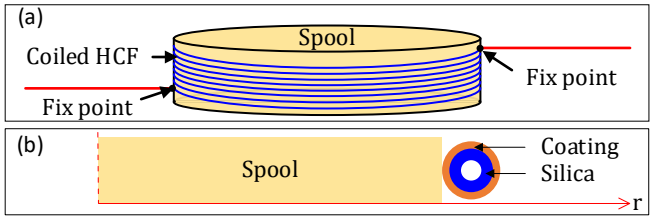

Fig. 1 (a) Schematic of the spooled HCF and (b) the 2D axisymmetric model in COMSOL Multiphysics (not to scale as the spool is significantly larger than the HCF).

In practice, there are several aspects that may reduce the effectiveness of this method. The most important is the coating that has very different mechanical and thermal properties to the glass and which will serve as a "cushion" between the spool and the glass fiber. To understand these effects, we performed simulation with Comsol Multiphysics.

We used a 2D axisymmetric model with the geometry shown in Fig. 1 (b). We neglect the mechanical properties of the HCF microstructure, approximating the HCF as a capillary. We consider it to be coated with a single acrylate coating. A contact boundary is applied between the HCF's outer surface and the coil. A body load in the direction of the spool center is applied to the HCF to simulate the effect of the stretching tension. For a spool radius R, the relationship between the body load F_L and the stretching tension F_T is:

$$F_L = -\frac{F_T}{R} \quad . \qquad \textbf{(1)}$$

In our simulations, we consider the spool to be made of Zerodur (Young's modulus 90.3 GPa), HCF of inner/outer diameter of 70/186 μm, made of silica (Young's modulus of 73.1 GPa and CTE = 0.3 ppm/K [15]), and coating with Young's modulus of 35 MPa and CTE = 180 ppm/K [16].

Firstly, we studied the influence of the HCF coating thickness. We considered a spool with R=75 mm and coating thickness of either 0 μm (bare HCF), 10 μm (thinly-coated HCF presented in [15] and used in our experiments), and 50 μm (typical thickness used, e.g., in [10]). As shown in Fig. 2, the uncoated and uncoiled HCF is expected to have a thermal sensitivity of 0.3 ppm/K, corresponding to the silica glass CTE. When coiled on the CTE = 0 spool, its thermal sensitivity is almost eliminated, in line with our expectations. For the uncoiled thinly-coated HCF, the coating slightly increases the HCF thermal sensitivity due to the significantly larger CTE of the coating relative to the silica glass. Thanks to the relatively low coating material stiffness (low Young's modulus) and small thickness, its effect on the overall HCF thermal sensitivity is very small, increasing the HCF thermal sensitivity by 0.05 ppm/K only. When coiled on the CTE = 0 spool, the HCF thermal sensitivity is strongly reduced, but it does not reach zero like for the uncoated HCF. However, the seven-fold reduction predicted is still significant For the standard-thickness coated HCF, the thermal sensitivity of the uncoiled HCF is relatively strongly influenced by the coating, increasing it ~1.5 times. When coiled on the CTE = 0 spool, the thermal sensitivity is reduced as in the previous two cases, but only by a factor of two.

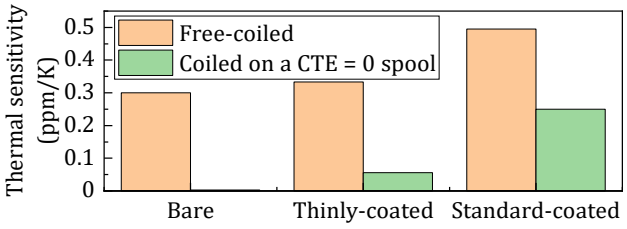

Fig. 2 Thermal sensitivity calculated for free-coiled HCFs (yellow) and spool-coiled HCFs (green) with different coating thickness (Bare, 0 μm; Thinly-coated, 10 μm; and Standard-coated, 50 μm).

Bare fibre is impractical (fragile) and standard-coated HCF (50 μm coating) does not show significant improvement when coiled on the CTE = 0 spool. Thus, with further simulations (and subsequent experimental demonstration) we focus on the thinly-coated HCFs.

Firstly, we analyze how the spool-coiled HCF thermal sensitivity changes with the HCF pre-stretching. By varying the pre-stretch force between 0 and 2 N we found that the HCF thermal sensitivity

is virtually insensitive to the pre-stretching. In the following simulations, we set this parameter to 0.5 N.

Further simulations revealed rather non-intuitive behaviours. Firstly, the thermal sensitivity of the spool-coiled HCF did not change significantly with the HCF silica thickness, while for an uncoiled HCF, thicker silica glass reduces the influence of the coating on the thermal sensitivity, Fig. 3.

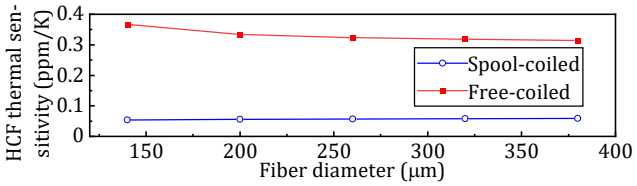

Fig. 3 Thermal sensitivity of spool-coiled HCF with respect to the fiber diameter and its comparison to free-coiled HCFs.

Further, we found that the Young's modulus of the coating had almost no influence on the thermal sensitivity of the spool-coiled HCF, while its CTE did, Fig. 4. This is very different to uncoiled HCFs, where the CTE × Young's modulus product influences the HCF thermal sensitivity (Eq. (2) in [15]). This suggests that the CTE = 0 spool-coiled HCF should have a coating with small CTE, irrespective of its Young's modulus. A candidate for such a coating is polyimide [17] used as fiber coating for high-temperature applications. In particular, Novastrat905 polyimide from NeXolve has a CTE close to 0 ppm/K.

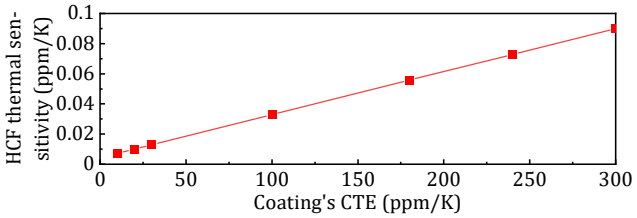

Fig. 4 Thermal sensitivity of spool-coiled HCF with respect to coating CTE.

Finally, we studied how the coiled HCF thermal sensitivity changes with the CTE of the spool material and the spool radius. Fig. 5 shows results for a CTE between -0.1 and 0 ppm/K, which is within the CTE range specified by Zerodur or ULE manufacturers (<± 0.1 ppm/K [13,14]). As expected, lower spool material CTE means a lower thermal sensitivity of the coiled HCF. We observe that the coiled HCF thermal sensitivity increases for smaller coil diameters. Our simulations confirmed this is due to the HCF thermal expansion in its cross-section, which increases the HCF centre circumference with temperature. The influence of this, however, reduces as the spool diameter increases, becoming negligible for infinitely-large spool. The data in Fig. 5 suggest a design rule for thermally-insensitive coiled HCFs. Firstly, we should target spools with a CTE between -0.1 and -0.05 ppm/K. Once the spool CTE is known, the spool diameter can be set to ensure zero-sensitivity coiled HCF (e.g., in Fig. 5, R = 44 mm gives zero HCF thermal sensitivity for a spool with CTE = -0.1 ppm, as does R = 82 mm for CTE = -0.05 ppm). Further tuning can be achieved by drilling a hole in the center of the spool, as this reduces its stiffness. This is shown in Fig. 6, where a coiled HCF thermal sensitivity of -0.02 ppm/K for a homogenous Zerodur spool with CTE = -0.05 ppm/K and R = 55 mm is tuned to zero sensitivity when a hole of 46 mm is drilled in the middle of the spool.

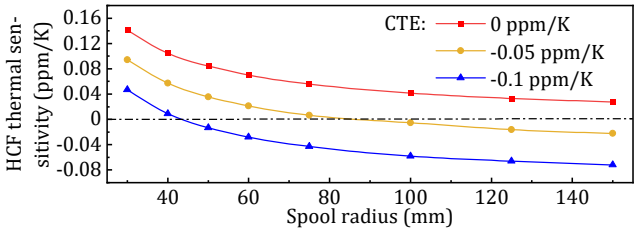

Fig. 5 Thermal sensitivity of coiled HCF with respect to the radius at different spool CTE values.

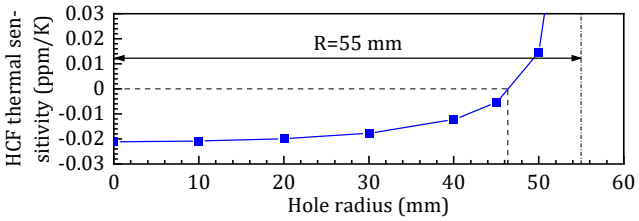

Fig. 6 Thermal sensitivity of coiled HCF on spool with CTE of -0.05 ppm/K with respect to the central hole radius for spool with R = 55 mm.

To demonstrate our method experimentally, we used a Zerodur cylinder with R = 75 mm that was salvaged from an old mirror, and a thinly-coated HCF (10 μm coating thickness) with an outer diameter of 206 μm [15]. Two HCF samples were prepared: one coiled on Zerodur (4.9-m long, fixed on the Zerodur spool with Capton tape), and one freely-coiled (4.4-m long). The HCF samples were each spliced with two mode-field adapters and SMF pigtails as described in [18]. At the HCF end-facets, there is 4% Fresnel reflection, as light travels from the solid glass core to the hollow core, forming the FPI.

The characterization set-up is shown in Fig. 7. Both HCF samples were put into a thermal chamber. The probe laser wavelength λ was locked to a carrier envelope offset stabilized Optical Frequency Comb to avoid any interference fringe instability due to any drift in laser wavelength. The signal was then split in two to enable probing of both interferometers at the same time. The HCF-FPI signals were observed in reflection (retrieved via two circulators), which gives better interference contrast in a low-finesse FPI than the transmitted signal.

The thermal chamber temperature was changed between 25 and 55°C. Fig. 8 shows how the reflection changed as a function of temperature for both HCF-FPIs. The reflected signal amplitude changes most likely because the polarisation state inside the HCF-FPIs changes with temperature. Each extrema corresponds to a phase change of π/2 and the thermal sensitivity can then be calculated by counting these extrema ($N_{extrema}$) observed over a temperature change of ΔT:

$$S_\phi = \frac{1}{\phi}\frac{d\phi}{dT} = \frac{N_{extrema}\cdot\lambda}{4\cdot\Delta T\cdot L}, \quad \textbf{(2)}$$

where L is the HCF length. The resulting thermal sensitivities are shown in Fig. 9. The result obtained for free-coiled HCF-FPI compares well to that simulated, also shown in Fig. 9. For the Zerodur-coiled HCF-FPI, we also get good agreement with simulations (also shown in Fig. 9) when we assume a Zerodur CTE of 0.07 ppm/K, which is within the manufacturer specification of <±0.1 ppm/K [13]. To further validate our model, we also analyzed results using a thickly-coated HCF measured in our preliminary report [12], achieving similar agreement with simulations as for the thinly-coated fibre presented here.

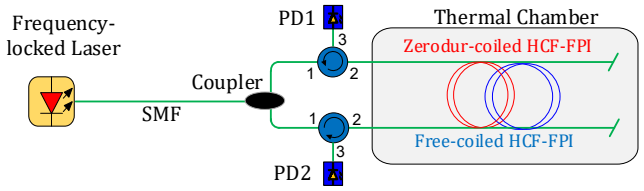

Fig. 7 Thermal sensitivity measurement setup using the free-coiled and zerodur-coiled HCF-FPIs.

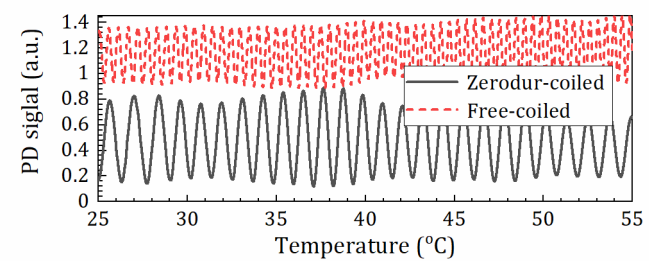

Fig. 8 Example measument of Zerodur-coiled HCF-FPI and free-coiled HCF-FPI.

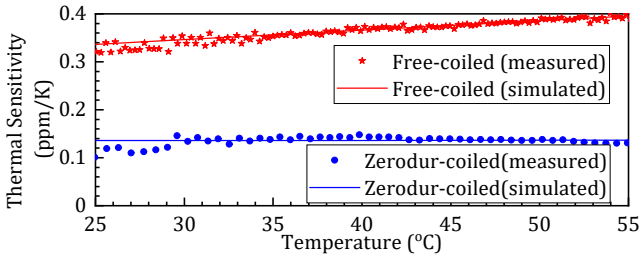

Fig. 9 Measured and simulated thermal sensitivities of Zerodur-coiled and free-coiled HCF-FPI. Simulations considered Zerodur CTE of 0.07 ppm/K.

Our experimental results show an improvement of the Zerodur-coiled HCF-FPI compared to the freely-coiled embodiment by a factor of three. However, we expect improvements by up to 7 times when using a coil with CTE = 0 and fully-insensitive HCF-FPI when selecting Zerodur with CTE = -0.06 ppm/K, which is within its specifications. Zerodur with selected specific CTE can be purchased from the manufacturer.

In conclusion, we analyzed a new method of achieving HCF-based FPIs with low and potentially even zero senstivity to temperature. Due to the HCF coating, zero thermal sensitivity requires a spool made of a material with negative CTE. Thinly-coated HCFs require a spool with only very small negative CTE (-0.1 to -0.05 ppm/K), which is available commercially (e.g., selected Zerodur or ULE materials). The HCF-FPI thermal sensitivity can be slightly tuned by controlling the spool and its central hole diameters, offering avenues to fine-tune the thermal sensitivity close to zero.

In our experimental demonstration we achieved a reduction of HCF-FPI thermal sensitivity by a factor of three, most probably limited by the CTE of the available spool. Even though we plan to further reduce its thermal sensitivity by using optimized spools, the achieved thermal sensitivity of 0.13 ppm/K is three times lower than the lowest value so far achieved at room temperature for any fiber FPI. Finally, we emphasize that the proposed method can be used in any optical fiber interferometer configuration.

Disclosures. The authors declare no conflicts of interest.

Data Availability. The data in this paper is accessible through the University of Southampton research repository [19]. For the purpose of open access, the authors have applied a creative common attribution (CC BY) license to any author accepted manuscript version arising.

REFERENCES

1. T. Kessler, C. Hagemann, C. Grebing, et.al. , Nat. Photonics. 6, 687-692 (2012).
2. S. Häfner, S. Falke, C. Grebing, et. al., Opt. Lett. 40, 2112-2115 (2015).
3. Luna, "FFPI Fibre Fabry-Perot Interferometer," (2020), https://lunainc.com/product/ffp-i.
4. W. Zhang, L. Stern, D. Carlson, et. al. , Laser Photonics Rev. 14, 1900293 (2020).
5. R. Slavík, G. Marra, E. N. Fokoua, et. al. , Sci. Rep. 5, 15447 (2015).
6. H. Sakr, T. D. Bradley, G. T. Jasion, et. al., in Optical Fiber Communication Conference (OFC) 2021, paper F3A.4.
7. M. Ding, E.R. Numkam Fokoua, T.D. Bradley, et. al. , J. Lightwave Technol. 39, 4489-4495 (2021).
8. M. Ding, M. Komanec, D. Suslov, et. al. , J. Lightwave Technol. 38, 2423-2427 (2020).
9. W. Zhu, E. R. Numkam Fokoua, Y. Chen, et. al. , Opt. Lett. 44, 2768-2770 (2019).
10. W. Zhu , Eric R. Numkam Fokoua, A. A. Taranta, et. al. , J. Lightwave Technol. 38, 2477-2484 (20251617).
11. R. Slavík, E. R. Numkam Fokoua, M. Bukshtab, et. al. , Opt. Lett. 44, 4367-4370 (2019).
12. M. Ding, E. R. Numkam Fokoua, T. D. Bradley, et. al. , in Conference on Lasers and Electro-Optics(2021), paper STu1Q.7.
13. Schott, "Thermal expansion of Zerodur," (2010), https://www.schott.com/en-gb/products/zerodur-p1000269.
14. Corning, "ULE Corning Code 7972 Ultra Low Expansion Glass," (2016), https://www.corning.com/media/worldwide/csm/documents/7972%20ULE%20Product%20Information%20Jan%202016.pdf.
15. B. Shi, H. Sakr, J. Hayes et. al., Opt. Lett. 46, 5177-5180 (2021).
16. DSM, "Product data for DeSolite 3471-3-14," (2019), https://focenter.com/wp-content/uploads/documents/AngstromBond---Fiber-Optic-Center-AngstromBond-DSM-3471-3-14-UV-Cure-FiberRe-Coating-(1Lt)-Fiber-Optic-Center.pdf.
17. C. Li, W. Yang, M.Wang, et. al. , Sensors 20(15): 4215 (2020).
18. M. Komanec, D. Suslov, S. Zvanovec, et. al. , IEEE Photon. Technol. Lett., 31, 723-726 (2019).
19. M. Ding, E.R. Numkam Fokoua, J.R. Hays, et al, Dataset, University of Southampton Institutional Repository (2022), https://doi.org/10.5258/SOTON/D2170.

Full Reference list:

1. T. Kessler, C. Hagemann, C. Grebing, T. Legero, U. Sterr, F. Riehle, M. J. Martin, L. Chen and J. Ye, "A sub-40-mHz-linewidth laser based on a silicon single-crystal optical cavity," Nat. Photonics. 6, 687-692 (2012).
2. Sebastian Häfner, Stephan Falke, Christian Grebing, Stefan Vogt, Thomas Legero, Mikko Merimaa, Christian Lisdat, and Uwe Sterr, "8 × 10−17 fractional laser frequency instability with a long room-temperature cavity," Opt. Lett. 40, 2112-2115 (2015)
3. Luna, "FFPI Fibre Fabry-Perot Interferometer," (2020), https://lunainc.com/product/ffp-i.
4. Wei Zhang, Liron Stern, David Carlson, Douglas Bopp, Zachary Newman, Songbai Kang, John Kitching, and Scott B. Papp "Observation of Gravitational Waves from a Binary Black Hole Merger", Laser Photonics Rev. 14, 1900293 (2020).
5. R. Slavík, G. Marra, E. N. Fokoua, N. Baddela, N. V. Wheeler, M. Petrovich, F. Poletti, and D. J. Richardson, "Ultralow thermal sensitivity of phase and propagation delay in hollow core optical fibers," Sci. Rep. 5, 15447 (2015).
6. H. Sakr, T. D. Bradley, G. T. Jasion, et. al., "Hollow Core NANFs with Five Nested Tubes and Record Low Loss at 850, 1060, 1300 and 1625nm," in Optical Fiber Communication Conference (OFC) 2021, paper F3A.4.
7. Meng Ding, Eric R. Numkam Fokoua, Thomas D. Bradley, Francesco Poletti, David J. Richardson, and Radan Slavík, "Finesse Limits in Hollow Core Fiber based Fabry-Perot interferometers," J. Lightwave Technol. 39, 4489-4495 (2021).
8. Meng Ding, Matěj Komanec, Dmytro Suslov, Daniel Dousek, Stanislav Zvánovec, Eric R. Numkam Fokoua, Thomas D. Bradley, Francesco Poletti, David J. Richardson, and Radan Slavík, "Long-Length and Thermally Stable High-Finesse Fabry-Perot Interferometers Made of Hollow Core Optical Fiber," J. Lightwave Technol. 38, 2423-2427 (2020).
9. W. Zhu, E. R. Numkam Fokoua, Y. Chen, T. Bradley, M. N. Petrovich, F. Poletti, M. Zhao, D. J. Richardson, and R. Slavík, "Temperature insensitive fiber interferometry," Opt. Lett. 44, 2768-2770 (2019).
10. W. Zhu , Eric R. Numkam Fokoua, A. A. Taranta, Y. Chen, T. Bradley, M.N. Petrovich ,F. Poletti , M. Zhao , D. J. Richardson , and R. Slavík, "The Thermal Phase Sensitivity of Both Coated and Uncoated Standard and Hollow Core Fibers Down to Cryogenic Temperatures," J. Lightwave Technol. 38, 2477-2484 (2020).
11. R. Slavík, E. R. Numkam Fokoua, M. Bukshtab, Y. Chen, T. D. Bradley, S. R. Sandoghchi, M. N. Petrovich, F. Poletti, and D. J. Richardson, "Demonstration of opposing thermal sensitivities in hollow-core fibers with open and sealed ends," Opt. Lett. 44, 4367-4370 (2019).
12. M. Ding, E. R. Numkam Fokoua, T. D. Bradley, F. Poletti, D. J. Richardson, and R. Slavík, "Hollow core fiber temperature sensitivity reduction via winding on a thermally-insensitive coil," in Conference on Lasers and Electro-Optics(2021), paper STu1Q.7.
13. Schott, "Thermal expansion of Zerodur," (2010), https://www.schott.com/en-gb/products/zerodur-p1000269.
14. Corning, "ULE Corning Code 7972 Ultra Low Expansion Glass," (2016),https://www.corning.com/media/worldwide/csm/documents/7972%20ULE%20Product%20Information%20Jan%202016.pdf.
15. Bo Shi, Hesham Sakr, John Hayes, Xuhao Wei, Eric Numkam Fokoua, Meng Ding, Zitong Feng, Giuseppe Marra, Francesco Poletti, David J. Richardson, and Radan Slavík, "Thinly coated hollow core fiber for improved thermal phase-stability performance," Opt. Lett. 46, 5177-5180 (2021).
16. DSM, "Product data for DeSolite 3471-3-14," (2019), https://focenter.com/wp-content/uploads/documents/AngstromBond---Fiber-Optic-Center-AngstromBond-DSM-3471-3-14-UV-Cure-FiberRe-Coating-(1Lt)-Fiber-Optic-Center.pdf.
17. Li, Changxu, Wenlong Yang, Min Wang, Xiaoyang Yu, Jianying Fan, Yanling Xiong, Yuqiang Yang, and Linjun Li, "A Review of Coating Materials Used to Improve the Performance of Optical Fiber Sensors," Sensors 20(15): 4215 (2020).
18. M. Komanec, D. Suslov, S. Zvanovec, Y. Chen, T. Bradley, S.R. Sandoghchi, E.R. Numkam Fokoua, G.T. Jasion, M.N. Petrovich, F. Poletti, D.J. Richardson and R.Slavik, "Low-Loss and Low-Back-Reflection Hollow-Core to Standard Fiber Interconnection," IEEE Photon. Technol. Lett., 31, 723-726 (2019).
19. M. Ding, E.R. Numkam Fokoua, J.R. Hays, et al, "Dataset for 'Hollow core fiber Fabry-Perot interferometers with reduced sensitivity to temperature'", University of Southampton Institutional Repository (2022), https://doi.org/10.5258/SOTON/D2170.